

University of Groningen

Tuning of the luminescence in poly((silanylene)thiophene)s

Herrema, Jan Karst

IMPORTANT NOTE: You are advised to consult the publisher's version (publisher's PDF) if you wish to cite from it. Please check the document version below.

Document Version

Publisher's PDF, also known as Version of record

Publication date:

1996

[Link to publication in University of Groningen/UMCG research database](#)

Citation for published version (APA):

Herrema, J. K. (1996). *Tuning of the luminescence in poly((silanylene)thiophene)s*. s.n.

Copyright

Other than for strictly personal use, it is not permitted to download or to forward/distribute the text or part of it without the consent of the author(s) and/or copyright holder(s), unless the work is under an open content license (like Creative Commons).

The publication may also be distributed here under the terms of Article 25fa of the Dutch Copyright Act, indicated by the "Taverne" license. More information can be found on the University of Groningen website: <https://www.rug.nl/library/open-access/self-archiving-pure/taverne-amendment>.

Take-down policy

If you believe that this document breaches copyright please contact us providing details, and we will remove access to the work immediately and investigate your claim.

Downloaded from the University of Groningen/UMCG research database (Pure): <http://www.rug.nl/research/portal>. For technical reasons the number of authors shown on this cover page is limited to 10 maximum.



CHAPTER 3

Synthesis, characterization and molecular structures of sila(2,5)thiophenophanes

ABSTRACT

Synthetic routes to a series of sila(2,5)thiophenophanes having thiophene rings bridged by permethyloligosilanes are presented. NMR spectra indicate that the phane compounds are dynamic in solution. The UV absorption spectra of the cyclic tetramers are fairly similar to analogous linear oligo[(silanylene)thiophene]s.

We studied the bulk molecular structures of four silathiophenophanes by means of X-ray diffraction. X-ray structure analysis of the phanes revealed no unexpected features. Bond lengths and angles and coplanarity of the thiophene rings of all four compounds indicate that the macrocycles are free of ring strain. The conformation of the macrocycles is determined on the one hand by a tendency to maximal molecular compactness and on the other hand by packing conditions in the crystal. For one of the phane compounds, viz. hexadecamethyloctasila[4.4]-(2,5)thiophenophane we also studied the surface molecular structure with scanning force microscopy. The AFM measurements demonstrate that intermolecular spacings on the surface correspond with those in the bulk.

3.1 INTRODUCTION

The cyclic sila(2,5)thiophenophanes are part of the family of 'phane' compounds, which comprise all bridged aromatics.¹ The most common aromatic unit inphanes is the benzene ring (this is indicated by the prefix cyclo). The first cyclophane ([2.2]metacyclophane) was already discovered in 1899.² An advance in cyclophane chemistry was introduced by Cram and Steinberg, when they published the first 'directed' synthesis of [2.2]paracyclophane³ in 1951. Phane compounds have been intensively studied because of the intriguing physical and chemical properties arising from through-space and through-bond interactions between separated π -systems. For instance, it has been demonstrated that aromatic rings in many cyclophanes are not planar, which has spectroscopic and chemical consequences. Cyclophane chemistry has become a major component of supramolecular chemistry, calixarenes,⁴ of models for intercalation, receptor models, crown ethers etc. For polymer chemists interesting compounds are strained cyclics that can act as monomers for ring-opening polymerizations.⁵ Cyclophane chemistry depends upon the three-dimensional geometry of its molecules. Therefore they are interesting model compounds because of special molecular and spectroscopic properties.

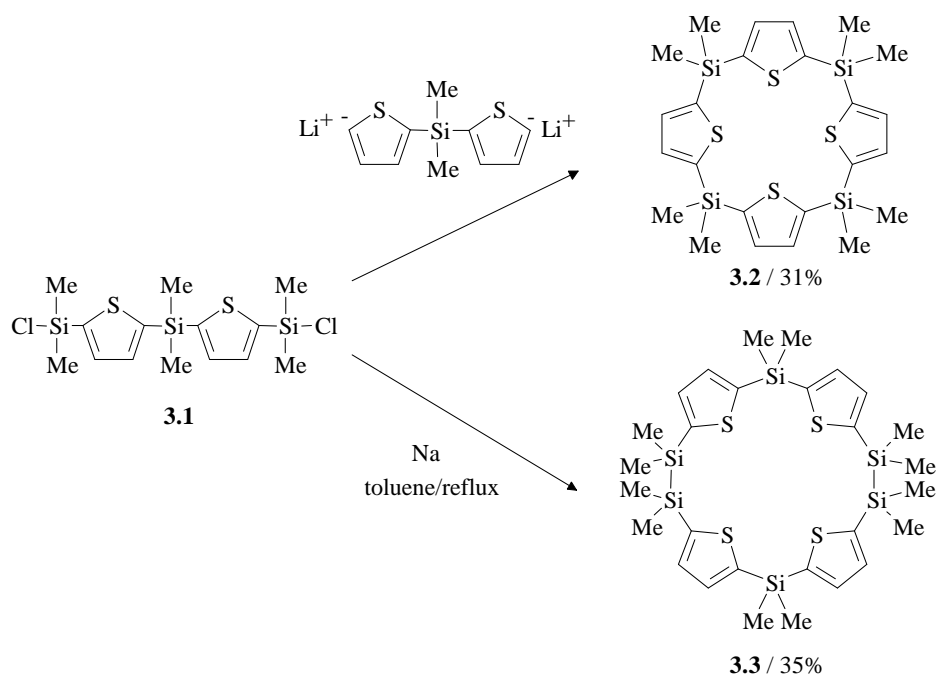
In this chapter we would like to demonstrate the synthesis and characterization of a series of compounds having thiophene rings bridged by methylated oligosilanes. In Chapter 5 the synthesis and characterization of poly[(silanylene)thiophene]s will be described. Along with the formation of linear copolymers⁶ a competitive process, macrocyclization, appeared in several syntheses. We could isolate cyclic products in yields varying from <1-5%. The silathiophenophanes presented here are new, except for octamethyltetrasilal[1.4](2,5)thiophenophane.⁷ We optimized the yield of these cyclic 'by-products' for some selected silathiophenophanes for the following reasons. For theoretical calculations on the geometry of (co)polymers the availability of precise X-ray data of model compounds and oligomers is valuable. These X-ray data can be used to verify the input of bond lengths and angles used for calculating electronic structures of copolymers such as performed by Ueda et al.⁸ for a series of poly[(disilanylene)thiophene]s. Secondly, cyclic compounds have constrained geometries which implies that analysis of UV absorption spectra and theoretical calculation is facilitated. And thirdly, these silathiophenophanes are in principle candidates for the formation of (transition) metal complexes.

3.2 RESULTS AND DISCUSSION

3.2.1 Synthesis.

The approach to optimizing the yields of the macrocyclic compounds is based on the dilution principle, which is the most important route for the synthesis ofphanes.⁹ Cyclizations taking advantage of the dilution principle usually start with open-chained educt compounds bearing two or more functional groups, and only the monomeric cyclization product is desired as the main product. The preference of the

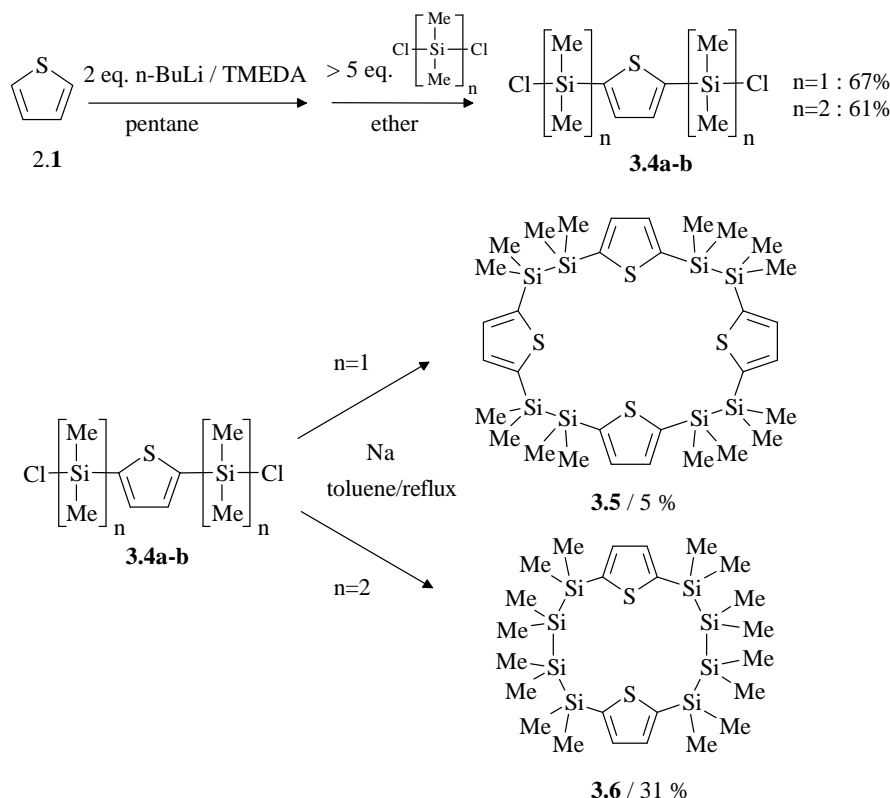
monomer formation is not simply based on the use of a large solvent volume and/or addition of highly diluted reagents. On the contrary, not the total amount of the solvent volume is decisive, but instead the establishment of a stationary concentration of the educts in the reaction flask that is as low as necessary. The dilution principle is very often used empirically, in our case too. The route for the synthesis of the cyclic compounds octamethyltetrasila[1.1.1.1](2,5)thiophenophane (**3.2**) and dodecamethylhexasila[1.2.1.2](2,5)thiophenophane (**3.3**) using the dilution principle is illustrated in Scheme 3.1. Synthesis of **3.2** was performed by adding together bis{5-[chloro-dimethylsilylene]-2-thienyl}dimethylsilane and the dilithio derivative of bis(2-thienyl)dimethylsilane. Synthesis and characterization of **3.2** had already been reported by Kauffmann and Kniese in 1973.⁷



Scheme 3.1 Reaction scheme for the synthesis of two silathiophenophanes by a metal-halogen exchange and Wurtz-coupling route respectively.

Apart from the cyclic tetramer obtained in 31% yield (after purification) some linear oligomers were found in the crude reaction mixture. Reaction conditions like concentration, solvent and addition time, were not further optimized because the quantities obtained were sufficient for characterization. Most probably the yield can be easily further improved by using THF instead of ether as a cosolvent. Chicart and coworkers reported the formation of a series of tetrasila[1.1.1.1](2,5)thiophenophanes (including **3.2** / 20% yield) having various substituents¹⁰ by reaction of dilithiothiophene and dichlorosilanes. The formation of these macrocyclic oligomers

was shown to be dependent on the solvent used. In particular, a polar solvent such as THF gave moderate to good quantities of cyclic oligomers. Another example of this solvent effect was reported by Lin and coworkers¹¹ for the synthesis of bisallenes. Condensation of Cl_2SiMe_2 and 1,3-dilithio-1,3-bis(trimethylsilyl)allene in Et_2O produced in 32% yield the polysilaallene and a trace of the cyclic compound 1,3,5,7-tetrakis(trimethylsilyl)-4,8-disilacycloocta-1,2,5,6-tetraene. The same condensation conducted in THF afforded the cyclic compound in 33% yield. Synthesis of **3.3** was performed using the Wurtz type coupling reaction. This Wurtz type coupling reaction for the formation of Si-Si bonds is widely used for the synthesis of polysilanes¹² and other polymeric materials containing disilanyl units.^{13,14,15,16} Just slowly adding the monomer **3.1** to a refluxing dispersion of sodium gave **3.3** in a reasonable yield of 35% compared to the 0.5 % using the conditions of the synthesis of the copolymer **5.1b**.



Scheme 3.2 Reaction scheme for the synthesis of a sila[4₂](2,5)thiophenophane and a sila[2₄](2,5)thiophenophane and their monomers.

Hu and Weber¹⁵ and Ishikawa and coworkers¹⁶ reported the synthesis of 2,5-bis(chlorodialkylsilyl)thiophenes by a three step method. We have prepared the monomers **3.4** in one step by reaction of thiophene with two equivalents of *n*-BuLi in the presence of *N,N,N',N'*-tetramethylethylenediamine (TMEDA) and subsequent reaction with excess dichlorotetramethyldisilane, and we have obtained good yields (Scheme 3.2). With hexane as solvent, the dilithio-intermediate is formed quantitatively.¹⁷ For reasons of solubility we used diethylether as a cosolvent. This probably results in a mixture of the mono- and di-lithiothiophene, which explains the somewhat lower yield. Slow addition of **3.4b** to an excess of sodium dispersion in boiling toluene gave the cyclic dimer **3.6** in 31% yield.

3.2.2 Characterization

NMR spectroscopy

The ¹H, ¹³C and ²⁹Si chemical shifts (CDCl₃) of the silathiophenophanes are compiled in Table 3.1. NMR spectra of the silathiophenophanes **3.2**, **3.5** and **3.6** display only one sort of protons for the thiophene rings in solution as sharp singlets indicating that these phane compounds are dynamic molecules in which the thiophene rings rapidly exchange positions. ¹H NMR spectra at low temperature (-70 °C, in CDCl₃ and hexane-*d*₁₄) did not reveal any presence of coalescence due to different conformers. Peak positions are consistent with the analogous linear compounds described in chapter 2 with the exception of a peak position of one of the thiophene signals of **3.3** found in the ¹H NMR at 6.96 ppm.

Table 3.1 NMR data of silathiophenophanes, recorded in CDCl₃

Cyclic	¹ H, δ, ppm		¹³ C, δ, ppm			²⁹ Si, δ, ppm
	Me	CH	Me	CH	C	
[TSiMe ₂] ₄ (3.2)	0.66	7.40	-0.3	135.4	144.9	-15.7
[TSi ₂ Me ₄] ₄ (3.5)	0.39	7.20	-2.8	135.8	143.3	-24.8
[TSi ₂ Me ₄ TSiMe ₂] ₂ (3.3)	0.44	6.96	-0.1	135.2	143.0	-24.5
	0.59	7.18	-3.0	136.5	144.0	-15.6
[TSi ₄ Me ₈] ₂ (3.6)	0.06	7.21	-1.8	135.0	145.0	-44.5
	0.37		-5.3			-20.7

UV-vis absorption spectroscopy

The UV absorption spectra of the silathiophenophanes **3.2**, **3.5** and **3.6** are plotted in Figure 3.1. For comparison some 'related' linear bisoligosilanylthiophenes are also included. The absorption λ_{max} values shift to longer wavelengths with increasing length of the oligosilylene block as was found for the linear model compounds. Both

[TSiMe₂]₄ (**3.2**) and [TSi₂Me₄]₄ (**3.5**) show a small red shift of the absorption spectrum in comparison with the linear bisoligosilanylthiophenes. In the case of **3.2** the presence of a shoulder on the long wavelength side is better visible. On the other hand, the absorption spectrum of octasila[4₂](2,5)thiophenophane (**3.6**) is blue shifted. The interaction of the Si-Si σ bonds with the π -system is not optimal due to the specific conformation of the cyclic (see paragraph 3.4).

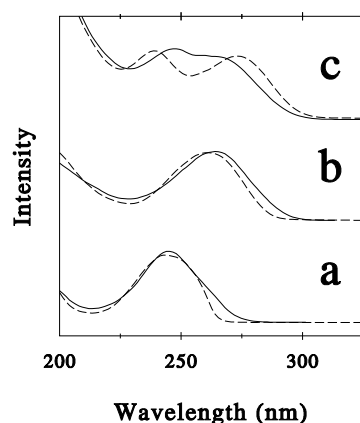


Figure 3.1

UV Absorption spectra of :

- (a) [TSiMe₂]₄ (**3.2**) [—] vs Me₃SiTSiMe₃ (**2.3a**) [---];
- (b) [TSi₂Me₄]₄ (**3.5**) [—] vs Me₅Si₂TSi₂Me₅ (**2.3b**) [---];
- (c) [TSi₄Me₈]₂ (**3.6**) [—] vs Me₉Si₄TSi₄Me₉ (**2.3c**) [---].

3.2.3 Molecular structures of silathiophenophanes¹⁸

For the silathiophenophanes **3.2**, **3.3** and **3.5** it has been possible to obtain single crystals suitable for crystal structure determinations. Although NMR and mass spectroscopy are powerful analytical techniques to identify compounds prepared in a synthetic route from indirect observations, X-ray crystallography is a far more powerful tool for a chemist in providing the conclusive proof of structure (in the solid state). The known X-ray structures of sil(an)yl-substituted 2-thiophene and 2,5-thiophene compounds: tetra(2-thienyl)silane¹⁹ and 5,5'-bis[dimethyl(2-thienyl)silyl]-2,2'-bithiophene,²⁰ both contain disorder. This results in anomalous bond lengths and bond angles for the thienyl ring. This is one of the reasons why the X-ray structures of the silathiophenophanes presented here which do not contain disorder, hold interesting and valuable information. Bond lengths, angles, torsion angles etc. can be the basis for the input for theoretical calculations on related copolymers. Furthermore, it can explain deviations from trends in e.g. UV absorption spectra of a series of compounds as will be illustrated here for compound **3.6**. The pertinent crystallographic data are summarized in Table 3.2 and some selected bond lengths and angles are collected in Tables 3.3-3.5.

Octamethyltetrasil[1₄](2,5)thiophenophane (**3.2**)

The cyclic tetramer **3.2** is found to be a centrosymmetric molecule in the crystal. It crystallizes in the monoclinic spacegroup P2₁/c analogous to the carbon variant, the

tetrathiaporphyrinogen.²¹ The four silicon atoms lie in a plane, from which the thiophene rings are tilted in the way dictated by the symmetry center by 8.0 and 73.0°, respectively. The shortest distance between the sulfur atoms - given for neighbouring thiophene rings in one cyclic - is 3.76 Å, which almost corresponds to twice the van-der-Waals radius of sulfur: 3.70 Å. The distance between sulfur atoms of the (almost coplanar) opposite thiophene rings which have their sulfur atoms directed inward, (S2 and S2') is slightly larger: 3.80 Å. A selection of bond lengths and angles is given in Table 3.3. The average Si-C distance for the carbon atom of the thiophene ring is 1.861 Å, which is slightly shorter than the 1.888 Å found in tetrathienylsilane. Bond lengths of the thiophene rings agree very well with those found for thiophene²² (1.714 Å, 1.370 Å, 1.423 Å). The contraction of *ca.* 3° of the S-C-C angle compared to 111.5° for thiophene is consistent with the analogous effect observed in e.g. [2.2](2,5)thiophenophane²³ and [1₄](2,5)thiophenophane²¹ where the angle of bridgehead atoms is also smaller. The thiophene rings are fully planar (C9, C10, C11, C12, S2), coplanar respectively (C3, C4, C5, C6, S1) within ±0.003 Å, indicating absence of ring strain. The dihedral angle between the two inequivalent thiophene rings is 107.6 °.

Table 3.2 Crystallographic data of compounds 3.2, 3.3 and 3.5.

Formula	C ₂₄ H ₃₂ S ₄ Si ₄ 3.2	C ₂₈ H ₄₄ S ₄ Si ₆ 3.3	C ₃₂ H ₅₆ S ₄ Si ₈ 3.5
<i>M</i>	561.12	677.43	793.75
Space group	<i>P</i> 2 ₁ / <i>c</i>	<i>P</i> $\overline{1}$	<i>P</i> $\overline{1}$
<i>a</i> /Å	6.564(2)	6.728(3)	7.972(1)
<i>b</i> /Å	12.455(1)	11.583(2)	10.747(1)
<i>c</i> /Å	18.057(3)	12.646(2)	13.428(1)
α /°	90	74.76(1)	83.33(1)
β /°	91.11(2)	87.79(2)	83.84(1)
γ /°	90	86.66(3)	85.31(1)
<i>V</i> /Å ³	1476.0	949.0(6)	1133.3(3)
<i>Z</i>	2	2	1
<i>D</i> _{calcd} /g cm ⁻³	1.263	1.185	1.163
<i>T</i> (K)	130	293	293
Crystal size /mm	0.15x0.15x0.4	0.3x0.35x0.3	0.4x0.3x0.2
μ (MoK α)/mm ⁻¹	0.48	0.44	0.43
Reflections measured	5089	3987	6149
Reflections <i>I</i> ≥ 3 σ (<i>I</i>)	3709	3471	3400
<i>F</i> (000)	296	360	424
<i>R</i>	0.033	0.039	0.043
<i>R</i> _w	0.037	0.040	0.046

A side view of the molecule projected along the direction passing through the silicon atoms is shown in Figure 3.2b. The packing found in the crystal structure, a so called herring-bone structure is illustrated in Figure 3.2c. The 'stacking' distance between the macrocyclics is fairly large, namely 6.56 Å.

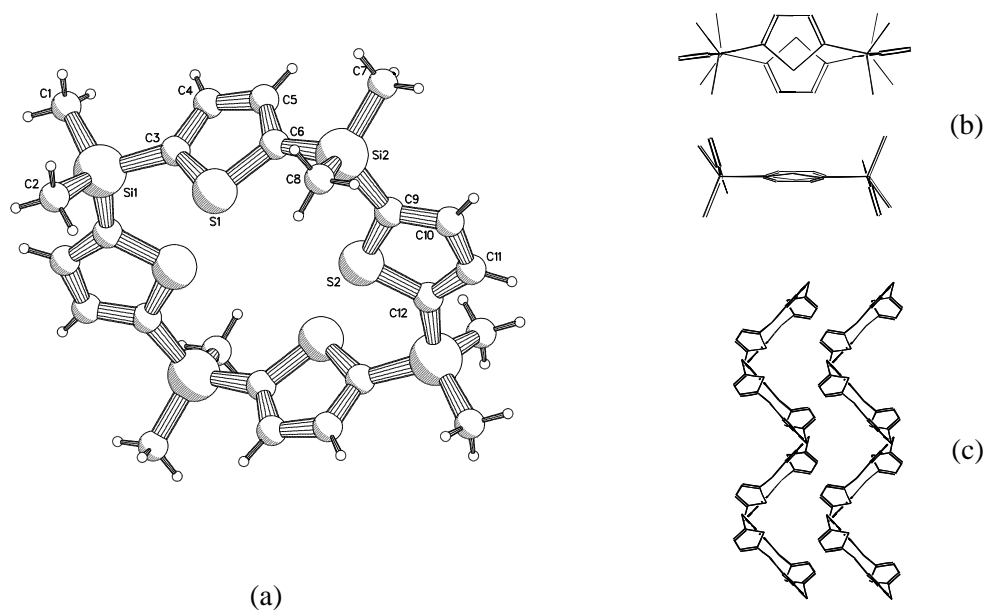


Figure 3.2 Structure of **3.2** in the crystal. (a) PLUTO drawing illustrating the conformation and the atom-numbering scheme. (b) Side views. (c) Topview of *ab*-plane.

Table 3.3 Relevant bond lengths (Å) and angles (°) of **3.2** with their esd's.

S(1)-C(3)	1.726(2)	C(4)-C(5)	1.418(3)
S(1)-C(6)	1.722(2)	C(5)-C(6)	1.374(3)
S(2)-C(9)	1.720(2)	C(9)-C(10)	1.384(3)
S(2)-C(12)	1.719(2)	C(10)-C(11)	1.420(3)
C(3)-C(4)	1.371(3)	C(11)-C(12)	1.380(3)
C(3)-S(1)-C(6)	94.51(9)	S(1)-C(6)-C(5)	108.9(1)
C(9)-S(2)-C(12)	94.42(9)	S(2)-C(9)-C(10)	109.1(1)
S(1)-C(3)-C(4)	108.7(2)	C(9)-C(10)-C(11)	113.7(2)
C(3)-C(4)-C(5)	114.1(2)	C(10)-C(11)-C(12)	113.4(2)
C(4)-C(5)-C(6)	113.8(2)	S(2)-C(12)-C(11)	109.4(1)

Dodecamethyltetrasilol[1.2.1.2](2,5)thiophenophane (3.3)

The X-ray structure analysis of **3.3** revealed no unexpected features. It crystallizes triclinic in the spacegroup $P\bar{1}$. The conformation of **3.3**, which is centro-symmetric like **3.2**, together with the atom-numbering scheme is shown in Figure 3.3. In contrast to the conformation of **3.2** all the thiophene rings are rotated in such a way that their sulfur atoms are disposed along the outer contour of the macrocycle.

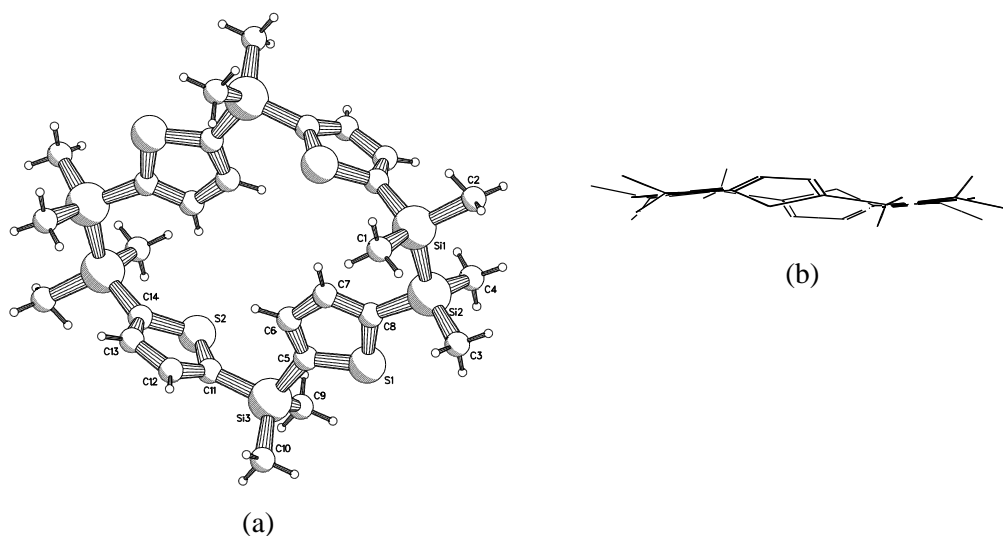


Figure 3.3 Structure of **3.3** in the crystal. (a) PLUTO drawing illustrating the conformation and the atom-numbering scheme. (b) Side view.

The orientation of the thiophene rings is probably determined on the one hand by a tendency to maximum molecular compactness (see Figure 3.3b) and on the other hand by packing conditions in the crystal. The intermolecular distances between the atoms are all longer than the van der Waals radii. A selection of bond lengths and angles is given in Table 3.4. Both thiophene rings are planar within ± 0.003 Å. The silicon atoms Si1, Si2 and Si3 lie almost in the plane of one of the thiophene rings (C5, C6, C7, C8, S1), being displaced 0.01-0.1 Å out of the plane. The dihedral angle between the two inequivalent thiophene rings is 80.5° .

Hexadecamethyltetrasilol[2.4](2,5)thiophenophane (3.5)

Figure 3.4a shows a drawing of a single molecule of **3.5**. The molecule has a center of symmetry. Cyclic **3.5**, like **3.3** has the thiophene rings rotated in such a way that their sulfur atoms are disposed along the outer contour of the macrocycle. The intermolecular distances between the atoms are all longer than the van der Waals radii. A selection of bond lengths and angles is given in table 3.5. Both thiophene rings are planar within ± 0.001 Å, ± 0.004 Å respectively. The dihedral angle between the two inequivalent thiophene rings is 38.2° .

Table 3.4 Relevant bond lengths (Å) and angles (°) of **3.3** with their esd's.

Si(1)-Si(2)	2.336(1)	C(6)-C(7)	1.412(4)
S(1)-C(5)	1.717(2)	C(7)-C(8)	1.365(3)
S(1)-C(8)	1.722(3)	C(11)-C(12)	1.350(3)
S(2)-C(11)	1.719(3)	C(12)-C(13)	1.417(4)
S(2)-C(14)	1.715(3)	C(13)-C(14)	1.359(4)
C(5)-C(6)	1.356(4)		
C(5)-S(1)-C(8)	94.9(1)	S(1)-C(8)-C(7)	107.9(2)
C(11)-S(2)-C(14)	94.6(2)	S(2)-C(11)-C(12)	108.5(2)
S(1)-C(5)-C(6)	108.6(2)	C(11)-C(12)-C(13)	114.5(3)
C(5)-C(6)-C(7)	114.2(2)	C(12)-C(13)-C(14)	113.7(2)
C(6)-C(7)-C(8)	114.4(3)	S(2)-C(14)-C(13)	108.7(2)

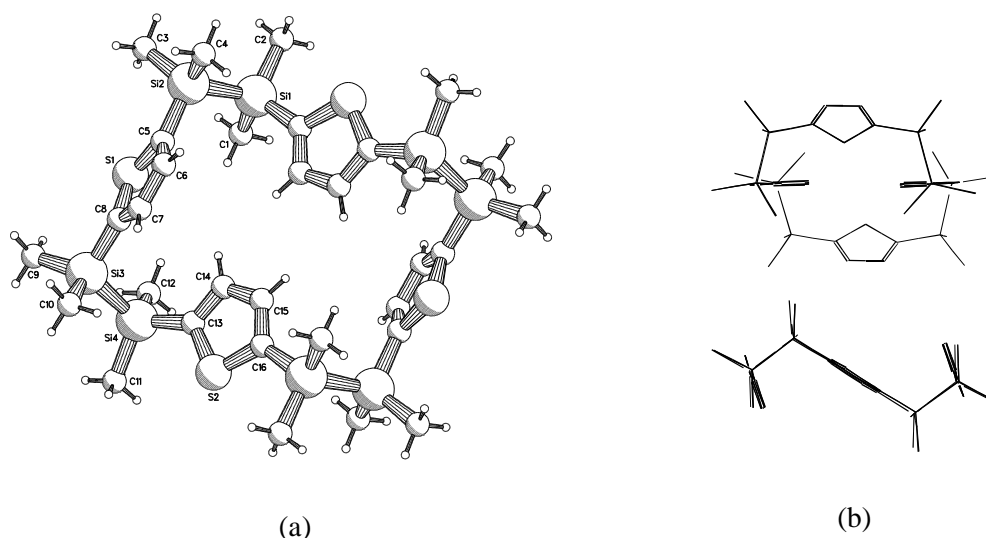


Figure 3.4 Structure of **3.5** in the crystal. (a) *PLUTO* drawing illustrating the conformation and the atom-numbering scheme. (b) Side and top view.

Discussion of the structures

The main difference between the structures of the three silathiophenophanes appears to be the conformation in the crystal, in particular the orientation of the thiophene rings, the S atoms being oriented inward or outward. As stated before, the orientation of the thiophene rings is probably determined on the one hand by a tendency to the maximum molecular compactness and on the other hand by packing

conditions in the crystal. Chemically inequivalent bond lengths and angles are compared in Table 3.6. As far as the bond lengths are concerned there are only minor differences among the three compounds. The bond angles of the thiophene rings seem to have small but consistent tendencies. This is possibly caused by overall ring-size of the cyclics or by π - σ conjugation going from **3.2** through **3.3** towards **3.5**.

Table 3.5 Relevant bond lengths (\AA) and angles ($^\circ$) of **3.5** with their esd's.

Si(1)-Si(2)	2.339(1)	C(5)-C(6)	1.359(5)
Si(3)-Si(4)	2.337(2)	C(6)-C(7)	1.419(5)
S(1)-C(5)	1.721(3)	C(7)-C(8)	1.358(5)
S(1)-C(8)	1.726(4)	C(13)-C(14)	1.366(5)
S(2)-C(13)	1.716(4)	C(14)-C(15)	1.417(6)
S(2)-C(16)	1.719(3)	C(15)-C(16)	1.348(3)
C(5)-S(1)-C(8)	94.9(2)	S(1)-C(8)-C(7)	108.0(3)
C(13)-S(2)-C(16)	95.2(2)	S(2)-C(13)-C(14)	108.1(3)
S(1)-C(5)-C(6)	108.3(3)	C(13)-C(14)-C(15)	113.6(4)
C(5)-C(6)-C(7)	114.2(3)	C(14)-C(15)-C(16)	115.1(3)
C(6)-C(7)-C(8)	114.6(3)	S(2)-C(16)-C(15)	108.0(3)

Table 3.6 Average bond lengths (\AA), angles and torsion angles ($^\circ$) of **3.2**, **3.3** and **3.5**

	3.2 [TSiMe ₂] ₄	3.3 [TSiMe ₂ TSi ₂ Me ₄] ₂	3.5 [TSi ₂ Me ₄] ₄		3.2	3.3	3.5
Si-Si	-	2.336	2.338	S-C-C (T)	109.0	108.4	108.1
S-C	1.722	1.718	1.720	C-C-C (T)	113.8	114.2	114.4
C=C	1.377	1.358	1.358	C-S-C	94.5	94.8	95.1
C-C	1.419	1.415	1.418	S-C-Si	124.0	122.5	123.3
Si-C(T) ^a	1.862	1.852	1.864	Si-C-C (T)	127.8	129.0	128.5
Si-C(Me) ^b	1.862	1.865	1.864	C-Si-Si-C	-	51	48/65

^aT = thiophene ring carbon atom(s); ^bMe = Methyl.

3.2.4 Molecular and surface structure of hexadecamethyloctasila[4.4]-(2,5)thiophenophane

The molecular structure of hexadecamethyloctasila[4.4](2,5)thiophenophane is shown in Figure 3.5. The X-ray structure is highly symmetric with a centre of symmetry. The thiophene rings are planar within 0.006 Å. The average bond lengths in the thiophene ring (1.725(10) Å, 1.415(4) Å, 1.381(10) Å) are in good agreement with the values found for thiophene (1.714 Å, 1.423 Å, 1.370 Å). The Si-Si bond lengths have normal values (2.34 Å). A comparison of the bond lengths and angles of $[\text{TSi}_4\text{Me}_8]_2$ with that of a planar thiophene ring indicate that the $[\text{TSi}_4\text{Me}_8]_2$ ring is almost strainless. The dihedral angle: Si-Si-Si-Si is 158.7°. This is very close to the preference of the energy minimum (160-170°) associated with the *trans* state calculated for a $[-\text{Si}(\text{CH}_3)_2-]_n$ model compound (MNDO/2).²⁴

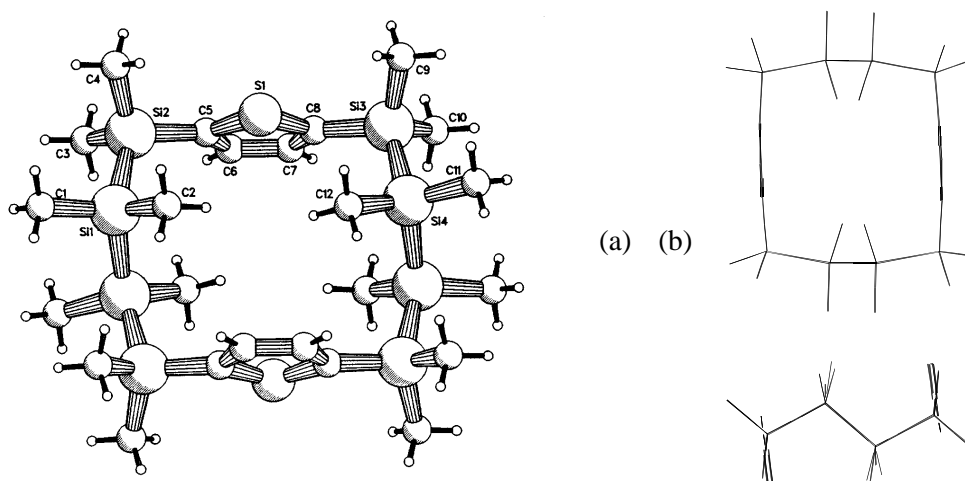


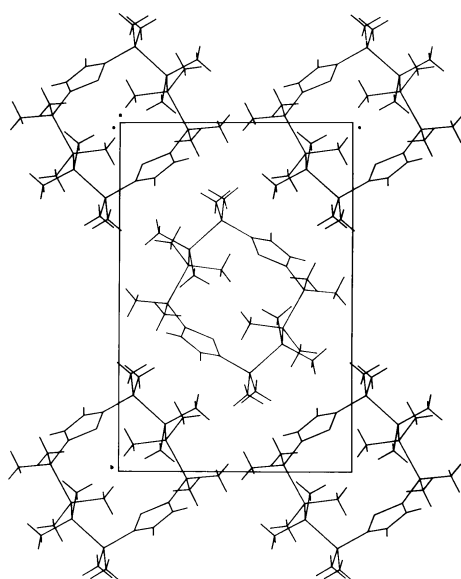
Figure 3.5 (a) PLUTO drawing of 3.6 illustrating the configuration and the atom-numbering scheme. (b) Side and top view.

Table 3.7 Crystallographic data for $[\text{TSi}_4\text{Me}_8]_2$ (3.6)

Formula	$\text{C}_{24}\text{H}_{52}\text{S}_2\text{Si}_8$	$D_{\text{calcd}} / \text{g cm}^{-3}$	1.114
<i>M</i>	629.5	$\mu(\text{MoK}\alpha) / \text{mm}^{-1}$	0.4
Space group	$P2_1/n$	Reflections measured	4507
<i>a</i> /Å	7.980(1)	Reflections $I \geq 3\sigma(I)$	3844
<i>b</i> /Å	18.797(2)	$F(000)$	680
<i>c</i> /Å	12.528(1)	<i>R</i>	0.032
β /°	93.38(1)	R_w	0.047
<i>V</i> /Å ³	1875.9(4)	Crystal size / mm	0.5x0.4x0.4
<i>Z</i>	2		

Table 3.8 *Relevant bond lengths (Å) and angles (°) of 3.6 with their esd's.*

Si(1)-Si(2)	2.347(1)	C(5)-C(6)	1.375(4)
Si(3)-Si(4)	2.337(1)	C(6)-C(7)	1.415(4)
S(1)-C(5)	1.733(2)	C(7)-C(8)	1.387(4)
S(1)-C(8)	1.717(2)		
C(5)-S(1)-C(8)	94.4(1)	C(6)-C(7)-C(8)	114.1(2)
S(1)-C(5)-C(6)	109.1(2)	S(1)-C(8)-C(7)	108.8(2)
C(5)-C(6)-C(7)	113.6(2)		

**Figure 3.6** *Projected packing plot of the molecules 3.6 in the unit cell viewed down the a-axis.***Surface structure with AFM.**^{24,25}

The atomic force microscope (AFM) produces images of topography of conducting and non-conducting materials by scanning a sharp tip mounted on a cantilever-type spring over a sample surface. The spring deflects in response to its interactions with surface features. The spring deflection is monitored with electron tunneling, optical interference, deflection of a laser beam, or capacitance detection. Typical resolution is on the nanometer and ångström scale. Since the first demonstration of atomic force microscopy in 1986,²⁶ surface structures of crystalline materials have been investigated by many groups worldwide. With AFM it is feasible to produce a surface molecular structure of organic molecules. In certain organic crystals a rearrangement of the molecules is observed producing a surface structure different from the bulk structure.^{27,28}

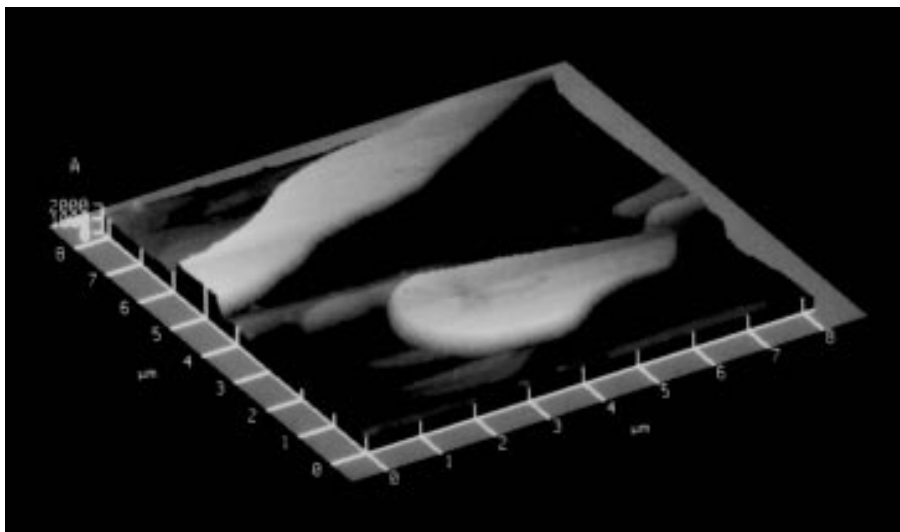


Figure 3.7 Large scale 3-D AFM image. Area $8.2 \times 8.2 \mu\text{m}$, constant force mode.

This paragraph presents the results of an AFM study of the surface structure of $[\text{TSi}_4\text{Me}_8]_2$ crystals. The crystals were grown via solvent evaporation of a 0.01 % $[\text{TSi}_4\text{Me}_8]_2$ solution in 1,2-dichlorobenzene and the crystal morphology was visualized with AFM. The molecular surface structure of the $[\text{TSi}_4\text{Me}_8]_2$ crystals is revealed with AFM and the high resolution image obtained is evaluated with a space filling model based on the crystallographic X-ray data.

The AFM imaging was started at a macroscopic level. Figure 3.7 shows a three dimensional AFM image of two parts of a $[\text{TSi}_4\text{Me}_8]_2$ crystal (area $8.2 \times 8.2 \mu\text{m}$). The crystal height determined by trace analysis is $980 \pm 50 \text{ \AA}$. Examination on a molecular scale produced the raw data AFM image given in Figure 3.8 (area $74 \times 74 \text{ \AA}$). It can be clearly seen that the surface structure shows regularity, but the image is distorted by superimposed high and low frequency noise. The low and high frequency noise was eliminated by Fast Fourier Transform filtering. The FFT option in the image process program, transforms the original AFM image in an 2-D inverse space image (2-D diffraction pattern). This 2-D diffraction pattern can be smoothed, to eliminate low and high frequency noise (removal of aperiodic component). After filtering the image can be transformed back to real space. The FFT filtered topview and 3-D AFM images are given in Figure 3.9. The molecular periodicity in the AFM image was determined with trace analysis. The periodicity in the x-direction is $12.52 \pm 0.26 \text{ \AA}$ and in the y-direction $7.82 \pm 0.19 \text{ \AA}$ (see Figure 3.9, x-direction: left \rightarrow right, y-direction: top \rightarrow bottom). The periodicities in the x- and y direction correspond with the dimensions of the c and a axis, of the monoclinic unit cell of $[\text{TSi}_4\text{Me}_8]_2$ ($a = 7.98 \text{ \AA}$, $b = 18.80 \text{ \AA}$, $c = 12.53 \text{ \AA}$, $\beta = 93.4^\circ$). So the surface structure of the crystal is most probably a representation of the (010) plane.

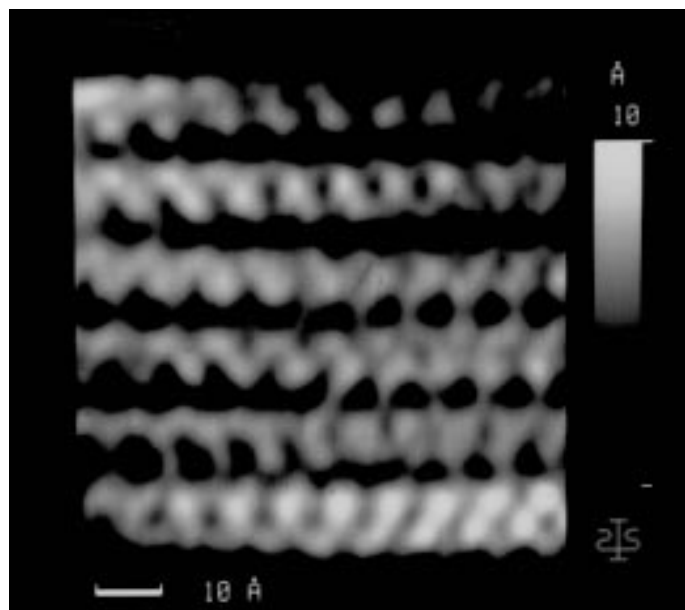


Figure 3.8 *Raw data AFM image of the surface structure of a $[\text{TSi}_4\text{Me}_8]_2$ crystal on a molecular scale: area $74 \times 74 \text{ \AA}$, constant force mode, scan rate 7.88 Hz.*

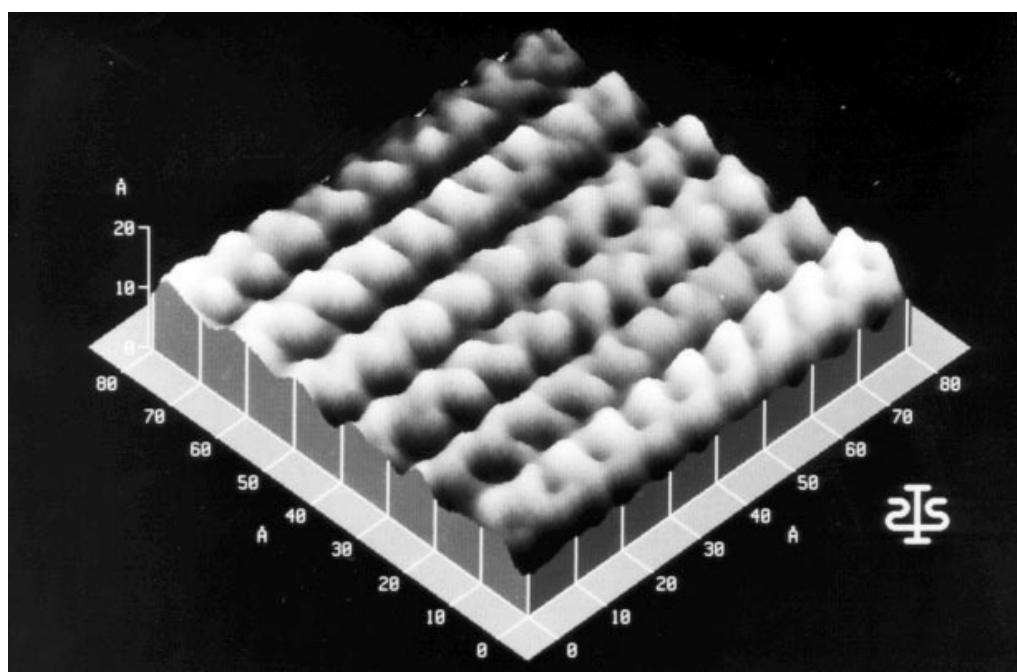


Figure 3.9 *AFM image as in Figure 3.8, three dimensional displayed after Fast Fourier Transform filtering (FFT): area $74 \times 74 \text{ \AA}$.*

A surface reconstruction of the (010) plane was made by linking nine unit cells together; a space filling representation is given in Figure 3.10. From this image it can be seen that the molecules are ordered in parallel rows along the a axis, with a side by side spacing of 12.53 Å. The molecular spacing within the rows is 7.98 Å. The $[\text{TSi}_4\text{Me}_8]_2$ rings are not at a right angle with the a axis, but are approximately 25° rotated (at an angle of 65° with the a axis). The topview AFM image shown in Figure 3.9 exhibits rotated features in the parallel rows. It is difficult to determine the average angle of these features with the a axis, because it seems that their orientation differs considerably between subsequent rows. A rough estimate of the angle with the a axis of $60\text{--}70^\circ$, determined from the upper two rows, is in reasonable agreement with the value of 65° determined from the space-filling model.

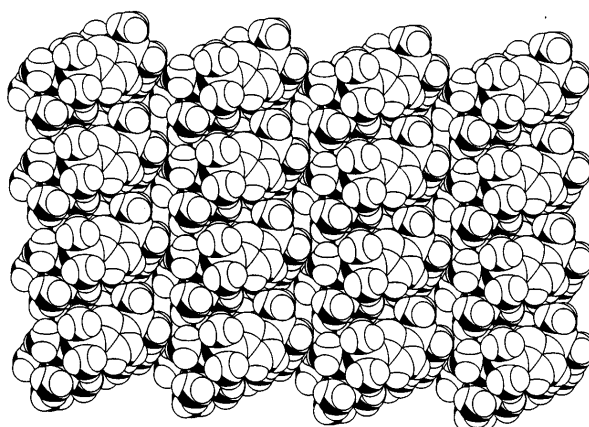


Figure 3.10 *Shaded top view of the a - c plane of 3×3 $[\text{TSi}_4\text{Me}_8]_2$ unit cells (PLUTO, space-filling model).*

A comparison between the two upper rows and the bottom row shows that the angles are opposite, suggesting that the bottom row is rotated 180° with respect to the upper rows. An aspect which is not clearly visible from the model is the relatively large depth of the gaps between the parallel rows, which is approximately 9.3 Å (half the length of the b axis). The relatively large depth of the gaps between the rows is clearly visible in the three dimensional AFM image shown in figure 3.9. Line trace analysis revealed that the depth of the gaps between parallel rows is approximately 5 - 6 Å. We can conclude that the molecular surface structure obtained with AFM on the top plane of a $[\text{TSi}_4\text{Me}_8]_2$ crystal is in good agreement with the space-filling model shown in Figure 3.10

3.3 CONCLUSIONS

In this chapter we have described the synthesis of a series of sila(2,5)-thiophenophanes. Both synthetic routes used, the condensation and the Wurtz coupling, gave cyclic compounds in fair to good yields. The conclusive proof of the structures was obtained by the use of X-ray structure analysis. The molecular structures confirmed the information obtained from NMR and UV absorption spectra. The phane compounds are free of ring strain and are flexible dynamic molecules in solution.

The molecular surface structure was revealed with Atomic Force Microscopy. A comparison of the AFM images with the crystallographic X-ray data showed that the scanned area is a representation of the (010) plane. The results for the crystallographic *a* and *c* axis of the monoclinic unit cell determined by atomic force microscopy are: $a = 7.82 \pm 0.19 \text{ \AA}$ and $b = 12.52 \pm 0.26 \text{ \AA}$ (X-ray analysis: $a = 7.89 \text{ \AA}$ and $c = 12.53 \text{ \AA}$).

3.4 EXPERIMENTAL

Atomic Force Microscopy

The $[\text{TSi}_4\text{Me}_8]_2$ crystals are prepared as follows: One drop of a 0.01 % solution of $[\text{T}(\text{SiMe}_2)_4]_4$ in 1,2-dichlorobenzene (Janssen Chimica) was spread on a clean 1 cm^2 silicon wafer. The wafer was stored in a 5 cm testtube to afford slow evaporation (three days). To ensure total evaporation of 1,2-dichlorobenzene, the sample was subsequently stored for two days in a vacuum oven (Heraeus VTR 5036) at 50°C . AFM measurements were performed on the Park Scientific Instruments AFM under ambient conditions in air, using a $10 \text{ }\mu\text{m}$ tube scanner and triangular shaped microfabricated Si_3N_4 levers with integrated tips ($L = 100 \text{ }\mu\text{m}$, $k = 0.34 \text{ N/m}$ and $\omega_t = 77 \text{ KHz}$). The tube scanner was calibrated (*x*, *y* direction) with a cleaved mica sample (hole to hole distance approximately 5.2 \AA).

X-Ray diffraction

The X-ray crystal structure analyses were performed at 130 and 293 K respectively using $\text{MoK}\alpha$ radiation on a Nonius CAD4F-diffractometer equipped with a graphite monochromator and interfaced to a VAX-730, using the θ - $2\theta^{30}$ technique. The structures were solved by direct methods.³¹ The remaining H-atoms could be revealed from a Fourier difference synthesis based on all the non H-atoms. Block-diagonal least-squares minimization of *F* with unit weights converged to the final *R* and *R_w* values, using anisotropic temperature factors for the non H-atoms. In the final refinement the H atoms were constrained to their corresponding C atoms at a distance of 0.96 \AA . A space-filling representation of the crystallographic *a-c* plane (consisting of nine linked unit cells) was made by A. Meetsma (PLUTO molecular modelling program).

Materials and Procedures

Bis{5-[chlorodimethylsilylene]-2-thienyl}dimethylsilane (3.1)

TMEDA (11.6 g, 0.1 mol) was added to a stirred solution of *n*-BuLi (40 mL, 0.1 mol). After 10 min. this BuLi/TMEDA solution was added to an ether solution (300 mL) of bis(2-thienyl)dimethylsilane (**2a**, 22.4 g, 0.1 mol). To the white suspension, another 70 mmol of *n*-BuLi was added without further cooling. The reaction mixture was refluxed for one hour, during which the white dilithium salt precipitated further. The suspension was slowly (45 min.) added

through a wide siphon to dimethyldichlorosilane (100 mL, 0.7 mol) at -30 °C in 50 mL of ether. The mixture was stirred for one hour at ambient temperature, decanted, and kugelrohr distilled (b.p. 200 °C, 1 mbar) yielding 34.6 g (83%) of **3.1** as a colourless viscous liquid.

¹H NMR δ 0.71 (s, 6H), 0.75 (s, 12H), 7.45 (d, 2H), 7.53 (d, 2H) ppm. ¹³C NMR δ -0.1/3.6 (Me), 136.6/136.8 (CH), 142.2/144.8 (C) ppm. ²⁹Si NMR δ -15.1/14.7.

Octamethyltetrasil[1₄](2,5)thiophenophane (3.2, [TSiMe₂]₄)

TMEDA (0.59 g, 5.2 mmol) was added to a solution of *n*-BuLi (4.1 mL, 10.2 mmol, 2.5 M in hexane). After 15 minutes this BuLi/TMEDA solution was added dropwise to an ether solution (15 mL) of bis(2-thienyl)dimethylsilane **2a** (1.12 g, 5 mmol) at 0 °C. During the reaction the white dilithium derivative of **2a** started to precipitate from the reaction mixture. After one hour at 25 °C this reaction mixture was added simultaneously with an ether solution (5 mL) of bis{5-[chlorodimethylsilyl]-2-thienyl}dimethylsilane (2.05 g, 5 mmol) to 25 mL of ether over a period of 30 minutes at r.t.. The reaction mixture was stirred for 3 hours, poured into 250 mL of a cold 5% NH₄Cl solution and extracted with methylene chloride (2 * 100 mL). The combined organic layers were washed with brine, dried (MgSO₄), filtered and concentrated to 15 mL, and pentane (20 mL) was added. Crystallization at -20 °C during one night afforded a mixture of oligomers and cyclic tetramer **3.2**, total yield 2.63 g (93%). Two further crystallizations from chloroform / pentane afforded pure octamethyltetrasil[1₄](2,5)thiophenophane, 0.84 g (1.5 mmol, 31%), mp. 284-286 °C. ¹H NMR δ 0.66 (s, 24H), 7.42 (s, 8H); ¹³C NMR δ -0.3 (Me), 135.4 (CH), 144.8 (C); ²⁹Si NMR δ -15.7 ppm. UV: λ_{max} = 243 nm, ε = 27800.

Dodecamethylhexasil[2.1.2.1](2,5)thiophenophane (3.3, [TSiMe₂TSi₂Me₄]₂)

In a 50 mL three-necked round bottom flask fitted with a reflux condenser, a pressure-equalizing capillary dropping funnel and a vibro stirrer, sodium (0.35 g, 15 mmol) and 40 mL of toluene were added. The contents of the flask were heated to reflux. To the 'vibro mixed' sodium dispersion obtained a solution of bis{5-[chlorodimethylsilylene]2-thienyl}dimethylsilane (2.05 g, 5 mmol) in 10 mL of toluene was slowly added dropwise. After vigorous stirring for another hour, the reaction mixture was cooled and added to a cold mixture of 10% aqueous NH₄Cl solution (25 mL) and isopropanol (50 mL). Another 100 mL of water was added and the aqueous solution was concentrated to some 20 mL. The resulting viscous material was decanted and dissolved in CH₂Cl₂, dried (MgSO₄) and concentrated. Flash column chromatography (kieselgel 60, CH₂Cl₂ / pentane 1/3) afforded **3.3**. Crystallization from CH₂Cl₂ / ether gave 0.59 g (0.87 mmol, 35%) as white crystals, mp 184-186 °C. Elemental analysis calcd for C₂₈H₄₄Si₈S₄: C, 49.64; H, 6.55. Found: C, 49.66; H, 6.56. ¹H NMR δ 0.44 (s, 24H), 0.59 (s, 12H), 6.96 (d, 4H), 7.18 (d, 4H); ¹³C NMR δ -3.0/-0.1 (Me), 135.2/136.5 (CH), 143.3/144.0 (C); ²⁹Si NMR -24.5/-15.6 ppm. UV: λ_{max} = 256 nm, ε = 94000.

2,5-Bis(dimethylchlorosilyl)thiophene (3.4a).

TMEDA (10.5 mL, 70 mmol) was added in 10 min. to *n*-BuLi (70 mmol, 2.5 M). The mixture was stirred for 15 minutes without cooling. After addition of 50 mL of pentane, thiophene (5.9 g, 70 mmol) was added in 15 min. at 0 °C. To the white suspension, another 70 mmol of *n*-BuLi was added at 0 °C, and stirred for another 30 minutes at room temperature. The suspension was slowly added through a wide siphon to dimethyldichlorosilane (420 mmol) at -40 to -20°C. The mixture was stirred overnight at ambient temperature. The solution was decanted, and kugelrohr distilled (b.p. 120 °C, 1 mbar) yielding 12.6 g (47 mmol, 67%) of **3.4a** as a colourless viscous liquid. ¹H NMR δ 0.72 (s, 12H), 7.48 (d, 2H); ¹³C NMR δ 3.2 (Me),

136.5 (CH), 143.3 (C); ^{29}Si NMR -24.5/-15.6 ppm.

2,5-Bis(1-chloro-1,1,2,2-tetramethyldisilanylene)thiophene (3.4b)

TMEDA (2.32 g, 20 mmol) was added to a stirred solution of *n*-BuLi (8.20 mL, 20 mmol). After 10 min the BuLi/TMEDA solution was added dropwise to a solution of thiophene (1.68 g, 20 mmol) in 50 mL of diethylether at -10 °C. A second equivalent of BuLi was added and the mixture was refluxed for one hour, during which the white dilithium salt precipitated. The suspension was added dropwise to an solution of dichlorotetramethyl-disilane (10 mL, 60 mmol) in 15 mL of diethylether at -30 °C. The solution was stirred at room temperature for 30 min, decanted, and the solvent was removed in vacuo. The residue was kugelrohr distilled (bp 150 °C/ 0.7 mm) yielding 4.65 g (12.1 mmol, 61%) of pure **3.4b**. ^1H NMR δ 0.49 (s, 12H), 0.51 (s, 12H), 7.36 (d, 2H).

Hexadecamethyltetrasil[2,4](2,5)thiophenophane (3.5, $[\text{TSi}_2\text{Me}_4]_4$)

For synthetic details see chapter 5. ^1H NMR δ 0.39 (s, 48H), 6.96 (s, 8H); ^{13}C NMR δ -2.8 (Me), 135.7 (CH), 143.2 (C); ^{29}Si NMR -24.7 ppm. UV: λ_{max} = 265 nm, ϵ = 107600.

Hexadecamethyloctasil[4,4](2,5)thiophenophane (3.6, $[\text{TSi}_4\text{Me}_8]_2$)

To a stirred dispersion of sodium (0.7 g, 30 mmol) in 50 mL of refluxing toluene (oil bath 150 °C) a solution of **3.4b** (3.85 g, 10 mmol) in toluene (10 mL) was added dropwise. The mixture was stirred vigorously for one hour, cooled with an ice-water bath and slowly added to a stirred mixture of 10% aqueous NH_4Cl solution (25 mL) and isopropanol (50 mL). The aqueous layer was concentrated in vacuo to a volume of 25 mL, decanted and the residue dissolved in chloroform, and dried (Na_2SO_4). Crystallization from chloroform/diethylether (1:10) afforded 0.68 g of **3.6**. Column chromatography (silica gel 60, CH_2Cl_2 / pentane 1:5) afforded another 0.3 g; total yield 0.98 g (1.56 mmol, 31%), mp 169-170 °C. Crystals suitable for an X-ray study were grown from ethanol. Elemental analysis calcd for $\text{C}_{24}\text{H}_{52}\text{S}_2\text{Si}_8$: C, 45.79; H, 8.33; S, 10.19. Found: C, 45.83; H, 8.18; S, 10.21. ^1H NMR δ 0.07 (s, 12H), 0.37 (s, 12H), 7.13 (s, 4H); ^{13}C NMR δ -1.8/-5.3 (Me), 135.0 (CH), 145.0 (C); ^{29}Si NMR -44.2/-21.0 ppm. UV: λ_{max} = 246 nm, ϵ = 27000. MS, *m/e* (rel intensity) 628 (M^+ , 20), 613 ($\text{M}^+ - \text{CH}_3$, 4).

3.5 REFERENCES

1. For a textbook on cyclophane chemistry see: Vögtle, F. *Cyclophane Chemistry: synthesis, structures and reactions*, John Wiley & Sons Ltd, Chichester, 1993.
2. Pellegrin, M.M. *Recl. Trav. Chim. Pays-Bas* **1899**, *18*, 457.
3. Cram, D. J.; Steinberg, H. *J. Am. Chem. Soc.* **1951**, *73*, 5691.
4. David Gutsche, C. *Calixarenes*, Royal Society of Chemistry: Cambridge, 1989.
5. Ishikawa, M.; Hatano, T.; Horio, T.; Kunai, A. *J. Organomet. Chem.* **1991**, *412*, C31-C33.
6. Wildeman, J.; Herrema, J.K.; Hadziioannou, G.; Schomaker, E. *J. Inorg. and Organomet. Pol.* **1991**, *1*, 567.
7. Kauffmann, T.; Kniese, H-H. *Tetrahedron Lett.* **1973**, *41*, 4043.
8. Tanaka, K.; Ago, H.; Yamabe, T.; Ishikawa, M.; Ueda, T. *Organometallics* **1994**, *13*, 3496.
9. (a) Rossa, L.; Vögtle, F. in *Topics in Current Chemistry 113, Cyclophanes I*, Boschke, F.L. (ed.) Springer-Verlag, Berlin Heidelberg, 1983. (b) For calculations of high dilution reactions see: Ercolani, G.; Mencarelli, P. *J. Chem. Soc., Perkin Trans. II* **1989**, 187. (c) Ercolani, G.; Mandolini, L.; Mencarelli, P. *J. Chem. Soc., Perkin Trans. II* **1990**, 747.

10. Chicart, P.; Corriu, R. J. P.; Moreau, J. J. E.; Garnier F.; Yassar, A. in *Chemistry of Synthetic High Polymers: Inorganic and Organometallic Polymers with Special Properties*, NATO ASI Ser., Ser. E 206; Kluwer: The Netherlands, 1992; p 179.
11. Lin, J.; Pang, Y.; Young, V.G.; Barton, T.J. *J. Am. Chem. Soc.* **1993**, *115*, 3794.
12. Miller, R.D.; Michl, J. *Chem. Rev.* **1989**, *89*, 1359
13. Nate, K.; Inoue, T.; Sugiyama, H.; Ishikawa, M. *J. Appl. Polym. Sci.* **1987**, *34*, 2445.
14. Ohshita, J.; Kanaya, D.; Ishikawa, M.; Yamanaka, T. *J. Organomet. Chem.* **1989**, *369*, C18.
15. Hu, S.; Weber, W.P. *J. Organomet. Chem.* **1989**, *369*, 155.
16. Oshita, J.; Kanaya, D.; Ishikawa, M.; Koike, T.; Yamanaka, T. *Macromolecules* **1991**, *24*, 2106.
17. Chadwick, D.J.; Willbe, C. *J. Chem. Soc., Perkin Trans. I* **1977**, 887.
18. For an excellent textbook for non-specialists on the general principles of crystal structure analysis and terminology see: Glusker, J.P., *Crystal structure analysis for chemists and biologists*, VCH Publishers: New York, 1994.
19. Karipedes, A.; Reed, A.T.; Thomas, R.H.P. *Acta Cryst.* **1974**, *B30*, 1372.
20. Lipka, A.; von Schnering, H.G. *Chem. Ber.* **1977**, *110*, 1377.
21. Vogel, E.; Röhrig, P.; Sicken, M.; Knipp, B.; Herrmann, A.; Pohl, M.; Schmickler, H.; Lex, J. *Angew. Chem., Int. Ed. Engl.* **1989**, *28*, 1651.
22. Bak, B.; Christensen, D.; Hansen-Nygaard, L.; Rastrup-Andersen, J. *J. Mol. Spectrosc.* **1961**, *7*, 58.
23. Pahor, N.B.; Calligaris, M.; Randaccio, L. *J. Chem. Soc., Perkin II* **1977**, 42.
24. Welsh, J.W.; Johnson, W.D. *Polym. Mat. Sci. & Eng.* **1989**, *61*, 222.
25. For general principles see: Grim, P.C.M. *PhD thesis*, University of Groningen, 1995.
26. For a review on STM and AFM in Organic Chemistry see: J. Frommer, *Angew. Chem., Int. Ed. Engl.* **1992**, *31*, 1298.
27. Binnig, G.; Quate, C.F.; Gerber, Ch. *Phys. Rev. Lett.* **1986**, *56*, 930.
28. Overney, R.M.; Howald, L.; Frommer, J.; Meyer, E.; Brodbeck, D.; Güntherodt, H.-J. *Ultramicroscopy* **1992**, *42-44*, 983.
29. Schulz, B.; Stiller, B.; Zetzsche, T.; Knochenhauer, G.; Dietel, R.; Brehmer, L. *Chem. Mater.* **1995**, *7*, 1041.
30. Nes, G.J.H. van; Bolhuis, F. van *J. Appl. Cryst.* **1978**, *11*, 206.
31. Computer Software: SDP/PDP (Enraf-Nonius and Frenz and Associates).